HHS Public Access

Author manuscript

Genes Chromosomes Cancer. Author manuscript; available in PMC 2016 August 31.

Published in final edited form as:

Genes Chromosomes Cancer. 2016 April ; 55(4): 340–349. doi:10.1002/gcc.22336.

Ewing Sarcoma With *ERG* Gene Rearrangements: A Molecular Study Focusing on the Prevalence of *FUS-ERG* and Common Pitfalls in Detecting *EWSR1-ERG* Fusions by FISH

Sonja Chen[1], **Kemal Deniz**[2], **Yun-Shao Sung**[1], **Lei Zhang**[1], **Sarah Dry**[3], and **Cristina R. Antonescu**[1,*]

[1]Department of Pathology, Memorial Sloan Kettering Cancer Center, NewYork, NY

[2]Department of Pathology, Erciyes University, Kayseri, Turkey

[3]Department of Pathology, UCLA, Los Angeles, CA

Abstract

The genetics of Ewing sarcoma (ES) are characterized by a canonical fusion involving *EWSR1* gene and a member of the ETS family of transcription factors, such as *FLI1* and *ERG*. In fact, *ERG* gene rearrangements represent the second most common molecular alteration, with *EWSR1-ERG* being identified in 5–10% of cases, while only a handful of reports document a *FUS-ERG* fusion. In this study, we focus on ES with *ERG* gene abnormalities, specifically to investigate the prevalence and clinicopathologic features of *FUS-ERG* fusions in a large cohort of small blue round cell tumors (SBRCTs) and compare to the eight reported *FUS*-positive ES. Among the 85 SBRCTs tested, seven (8.2%) cases harbored *FUS* gene rearrangements; six fused to *ERG* and one with *FEV*. During this investigation we came across a number of *ERG*-rearranged ES lacking both *EWSR1* and *FUS* abnormalities by FISH. In one case, RNA sequencing identified an *EWSR1-ERG* transcript despite the negative *EWSR1* rearrangements by FISH. Additional 3-color FISH fusion assay demonstrated the fusion of *EWSR1* and *ERG* signals in all four cases negative for break-apart *EWSR1* FISH. These results emphasize a potential pitfall of relying on *EWSR1* FISH assay alone for diagnosis of ES. In cases with classic morphology and/or strong CD99 and ERG immunoreactivity, additional molecular testing should be applied, such as *ERG* FISH or RT-PCR/next generation sequencing, for a more definitive diagnosis. Although our study group is small, there were no differences noted between the clinical, morphologic features and immunoprofile of the different subsets of *ERG*-rearranged SBRCTs.

INTRODUCTION

The genetic hallmark of Ewing sarcoma (ES) is the recurrent t(11;22)(q24;q12) translocation resulting in the fusion of *EWSR1* and *FLI1* genes, identified in 90% of cases (Delattre et al., 1992, 1994). The second most common molecular abnormality is the t(21;22)(q22;q12), which accounts for 5% of the cases, resulting in an *EWSR1-ERG* fusion (Ginsberg et al.,

*Correspondence to: Cristina Antonescu, MD, Department of Pathology, Memorial Sloan Kettering Cancer Center, 1275v York Ave, New York, NY 10065, USA. antonesc@mskcc.org.

Additional Supporting Information may be found in the online version of this article.

1999). Only a small subset of ES shows *EWSR1* fusions with other members of the ETS family of transcription factors, such as *ETV1* (7p22) (Jeon et al., 1995), *E1A-F* (17q21) (Kaneko et al., 1996) and *FEV* (2q35-36) (Peter et al., 1997).

In addition to these well-defined and relatively common genetic abnormalities, alternative fusions have been reported, with either *EWSR1* being fused to non-ETS partners or *FUS* substituting for *EWSR1* in its fusions with ETS transcription factors. In both categories, the number of cases reported has been relatively small (case reports or small series) and insufficient to draw definitive conclusions as to whether any of these genetic subgroups belong to the *EWSR1-ETS*-positive conventional ES or as separate pathologic entities. In the first group, four different non-ETS partners have been described, including two members of the zinc-finger family of proteins, *PATZ1* (Mastrangelo et al., 2000) and *SP3* (Wang et al., 2007), *NFATC2*, a member of the nuclear factors of activated T cells transcription complex (Szuhai et al., 2009) and *SMARCA5*, a chromatin-remodeling gene (Sumegi et al., 2011). *EWSR1* and *FUS* are members of the FET family of RNA binding proteins and presumed to have overlapping function as they can interchange in a number of translocation-associated sarcomas (Antonescu, 2014). However, only five cases of SBRCT with t(16;21)(q11.2;q22) resulting in *FUS-ERG* (Shing et al., 2003; Berg et al., 2009) and two cases harboring *FUS-FEV* fusions (Ng et al., 2007; Pierron et al., 2012) have been described to date.

In this study, we sought to investigate the prevalence of the *FUS-ERG* gene fusion in a large cohort of pathologically and molecularly well characterized SBRCTs, lacking other known gene rearrangements. Since most of the reported *FUS*-rearranged SBRCT have a limited pathologic description, we also carried out a detailed histologic and immunohistochemical analysis of these lesions, and compared to the reported cases.

MATERIALS AND METHODS

The files of the Pathology Department of MSKCC and personal consultation files (CRA) were reviewed for SBRCTs, in which material for molecular analysis was available. Criteria of selection for the study were tumors that were negative for *EWSR1*, *CIC*, and *BCOR-CCNB3* gene abnormalities by FISH. The clinical data were obtained from the medical records. Hematoxylin and eosin stained sections and immunohistochemical stains were re-evaluated in all cases. Tumors were reviewed for growth pattern, cell size, cytomorphology (round, oval, spindle, rhabdoid), nuclear features including contour, pleomorphism, chromatin pattern, presence of nucleoli, “starry sky” appearance, mitotic activity, and necrosis. The stromal component was also assessed for abundance and type (myxoid, collagenous). The study was approved by the Institutional Review Board 02-060.

Fluorescence In Situ Hybridization Analysis

FISH for break-apart assay was applied on formalin-fixed and paraffin-embedded 4-micron sections in all cases. FISH was performed by applying custom probes using bacterial artificial chromosomes (BACs), covering and flanking the *FUS*, *EWSR1*, *ERG*, and *FEV* genes. BAC clones were chosen according to the UCSC genome browser (http://genome.ucsc.edu), see Supporting Information Table 1. The BAC clones were obtained from the BACPAC sources of Children's Hospital of Oakland Research Institute (CHORI)

(Oakland, CA) (http://bacpac.chori.org). DNA from individual BACs was isolated according to the manufacturer's instructions, labeled with different fluorochromes in a nick translation reaction, denatured, and hybridized to pretreated slides. Slides were then incubated, washed, and mounted with DAPI in an antifade solution, as previously described (Antonescu et al., 2010). The genomic location of each BAC set was verified by hybridizing them to normal metaphase chromosomes. Two hundred successive nuclei were examined using a Zeiss fluorescence microscope (Zeiss Axioplan, Oberkochen, Germany), controlled by Isis 5 software (Metasystems, Newton, MA). A positive score was interpreted when at least 20% of the nuclei showed a break-apart signal. Nuclei with an incomplete set of signals were omitted from the score.

RNA Sequencing and Fusion Sequencing Data Analysis

In one case lacking *EWSR1*, *FUS*, *CIC*, and *BCOR-CCNB3* adequate RNA was available for RNA sequencing using paired-end sequencing for fusion gene discovery. Total RNA was prepared according to the Illumina mRNA sample preparation protocol (Illumina). Briefly, mRNA was isolated with oligo(dT) magnetic beads from total RNA (10 μg) followed by fragmentation at 94°C for 2.5 min in fragmentation buffer (Illumina). Prior to the adapter ligation step, an additional size-selection step (capturing 350–400 bp) was introduced to reduce inclusion of artifactual chimeric transcripts due to random priming of transcript fragments into the sequencing library (Quail et al., 2008). Enrichment of the adapter-ligated library was achieved by PCR for 15 cycles. After purification, the library was sized and quantified using DNA1000 Kit (Agilent) on an Agilent 2100 Bioanalyzer according to the manufacturer's instructions. Paired-end RNA-sequencing at read lengths of 50 to 51 bp was performed with the HiSeq 2500 (Illumina).

Data analysis of RNA Sequencing Results was performed with the FusionSeq algorithm. Reads were independently aligned with STAR alignment software against the human genome reference sequence (hg19) and a splice junction library, simultaneously (Dobin et al., 2013). After conversion of mapped reads into Mapped Read Format (Habegger et al., 2011), analysis was performed using FusionSeq (Sboner et al., 2010). Briefly, in a first step, paired end reads mapping to different genes were used to identify potential chimeric candidates. A cascade of filters, each taking into account different sources of noise in RNA-sequencing experiments, was then applied to remove spurious fusion transcripts. After generation of a confident list of fusion candidates, they were ranked to prioritize experimental validation (Sboner et al., 2010).

RESULTS

FUS-Rearranged Small Blue Round Cell Tumors

We screened a total number of 85 SBRCTs that were negative for gene abnormalities in *EWSR1*, *CIC*, and *BCOR* by FISH and found seven (8.2%) cases that showed *FUS* gene rearrangements. These cases were then screened for *ERG* gene abnormalities by FISH and found to be positive in six of the seven cases (Fig. 1). The remaining *ERG*-negative *FUS*-rearranged SBRCT was then screened for *FEV* gene abnormalities and was found to be positive (Fig. 1).

Clinicopathologic features of the seven *FUS*-rearranged SBRCT patients are summarized in Table 1. All patients except one were females, with a mean age 30.8 years (range 13–46, median 31). The anatomic site was distributed between bone and soft tissue of the extremities, with four and three cases, respectively. The skeletal tumors occurred in the chest wall, ilium, and distal femur, while the soft tissue lesions were deep seated in the arm and thigh.

Histologically, all *FUS*-rearranged SBRCTs showed a solid growth of monomorphic, mainly small-sized, round to oval neoplastic cells. Five of the six *FUS-ERG* positive tumors showed hyperchromatic nuclei (Figs. 1A–1C), while one case showed vesicular nuclei with small, inconspicuous nucleoli (Fig. 1D). Only one of the cases showed focal areas of spindling and focal myxoid changes (Figs. 1B and 1C). One case showed thick collagenous bands dividing the tumor in wide compartments (Figs. 1D and 1E). There was no significant nuclear pleomorphism in any of the cases, with only mild variation in size and shape, and mostly smooth nuclear borders. The tumor cells had indistinct cell borders, with mostly scant cytoplasm, ranging from clear, vacuolated to light eosinophilic. The mitotic count varied from 8 to 32/10HPFs, with a mean of 17.5 ± 10.2. Four cases showed geographic necrosis (Fig. 1E). The only *FUS-FEV* positive tumor showed a more abundant clear cytoplasm and had a diffusely myxoid background.

All seven *FUS*-rearranged SBRCT showed diffuse membranous staining for CD99 (Fig.1F). Focal positivity for CAM5.2 was seen in one case, while S100 protein was noted in two cases, one case (ES7) showing diffuse and strong reactivity (also co-expressing SOX10), while the other only focal reactivity (ES3).

Meta-Analysis of the Eight *FUS*-Rearranged SBRCTs Reported in the Literature

The clinicopathologic features of these eight ES patients harboring *FUS*-related fusions from the literature (Shing et al., 2003; Ng et al., 2007; Berg et al., 2009; Brohl et al., 2014) are summarized in Table 1. Clinicopathologic and immunohistochemical information for one of the cases was not available (Pierron et al., 2012). Of the remaining patients there were four males and three females, with a mean age of 14.7 years (range: 3–33 years; median 15). All except one were located in the bone, with three involving chest wall, two in the femur and one in the clavicle. The remaining case occurred in the kidney.

Histologically, the growth pattern reported varied among nodular/nested, solid/sheet-like, and infiltrative. None of the reported cases demonstrated a spindled appearance. Only one case was described displaying mild nuclear pleomorphism, while remaining showed a monomorphic cytologic appearance. Half of the cases showed necrosis, extensive in one and focal in two. Immunohistochemically, all except one displayed a diffuse membranous pattern of CD99 staining.

Of the two reported *FUS-FEV*-rearranged SBRCT, only one case had available clinical information. This SBRCT occurred in the clavicle of a 33-year-old male and showed diffuse strong membranous positivity for CD99 (Ng et al., 2007). Although no clinical information was available for the second reported case (Pierron et al., 2012), it was described as clinically and morphologically similar to ES.

A proportion of ERG-rearranged ES lack FISH abnormalities in EWSR1 and FUS genes

Among the 15 *ERG*-rearranged ES identified in our database, 4 (27%) lacked gene abnormalities in either *EWSR1* or *FUS* by FISH. The remaining cases showed *EWSR1* in four cases and *FUS* gene rearrangements in seven cases. The total number of *EWSR1-ERG* positive ES is under-represented in this cohort, since most *EWSR1*-rearranged ES with typical clinical and pathologic findings are not routinely screened to confirm its specific fusion partner (i.e., *FLI1* or *ERG*). Furthermore, the aim of this study was not designed to establish an accurate incidence of *EWSR1-ERG* fusion positive ES, but rather investigate the frequency and clinicopathologic characteristics of *FUS-ERG* positive cases. Despite this bias, these results point out an important pitfall in screening ES only with *EWSR1* FISH. In some of these cases *ERG* FISH testing was performed despite negative FISH results for both *EWSR1* and *FUS*, due to typical morphologic features and/or strong and diffuse reactivity for ERG immunoreactivity. Furthermore, in one case RNA sequencing was performed due to negative FISH results for all known fusions, including *EWSR1*, *FUS*, *CIC*, and *BCOR*, in an attempt to discover novel fusion genes. Only after the *EWSR1-ERG* fusion transcript was detected by FusionSeq and subsequently validated by RT-PCR, FISH was performed to confirm the *ERG* gene rearrangement (Fig. 2A).

FISH Fusion Assays Confirm the *EWSR1-ERG* Fusion in Cases with Negative *EWSR1* FISH Break-Apart Results

As *EWSR1* and *ERG* have opposite directions of transcription, the *EWSR1-ERG* fusion typically does not result through a simple balanced translocation, as seen with *EWSR1-FLI1* or *FUS-ERG* fusion. As shown in Figure 2, two breaks are required in the 22q12 locus resulting in *EWSR1* break and inversion before being inserted in 21q22.3. Depending on the distance between the two breaks in 22q12, the *EWSR1* break-apart FISH assay (red, centromeric; green, telomeric) may or may not detect the *EWSR1* gene rearrangements (Fig. 2B). As the resolution of FISH is suboptimal for breaks < 2 Mb apart, some of the smaller breaks/insertions in ES with *EWSR1-ERG* fusion are not detected by this method, the so-called “cryptic” *EWSR1-ERG* fusions. Thus, in order to confirm this result, we carried out a three-color FISH fusion assay: orange, *EWSR1* centromeric, green, *EWSR1* telomeric, and red, *ERG* centromeric BACs (Fig. 2C). Indeed, the remaining three cases with *EWSR1* negative FISH break-apart but positive for *ERG* rearrangement showed a fused red-orange signal, in keeping with a 5′ centromeric *EWSR1-ERG* fusion (Fig. 2C). Thus, a diagnosis of *EWSR1-ERG* positive ES was confirmed in all eight cases; clinical findings being summarized in Table 2. There were six females and two males, with a mean age at diagnosis of 15 years (range: 1–23; median 19). The tumors were more commonly located in the bone (ilium, spine, mandible), four cases, followed by soft tissue (retroperitoneum, intra-abdominal), two cases and one case each in the brain and scalp.

Histologically, the *EWSR1-ERG* positive ES were composed of uniform small round to oval neoplastic cells with scant light eosinophilic to vacuolated cytoplasm and indistinct cell borders. Four cases displayed solid growth, three had a nodular architecture (Figs. 3A and 3B), and one a nested appearance (Fig. 3C). Most cases showed a fine chromatin pattern (Fig. 3B), while two had vesicular nuclei with smooth nuclear contours. Only one tumor showed a coarser chromatin pattern with irregular nuclear membranes and a mild nuclear

pleomorphism. The mitotic count varied from 1 to 33/10 HPFs, with a mean of 11 ± 10.8. Most of the cases showed geographic or multifocal necrosis (5/8 cases), which in two was focal. The stromal component was typically scant, except for one brain tumor, showing extensive hyalinization without any prior treatment. None of the cases had myxoid stroma. All cases showed diffuse membranous staining for CD99 (Fig. 3D). FLI1 was positive in one case.

DISCUSSION

The histologic and molecular spectrum of the Ewing sarcoma (ES) family of tumors is still evolving since the initial description by Dr. James Ewing in 1921 (Ewing, 1921). Classic ES is characterized by a monotonous cytomorphology, with round nuclei, smooth nuclear contours, and fine to vesicular chromatin. Intra-tumoral architectural and cytologic heterogeneity is not a feature of classic ES. Atypical Ewing sarcoma was first described as a morphologic variant of classic ES in the 1970s, showing deviations from its typical monomorphic proliferation of primitive round cells (Llombart-Bosch et al., 1978), such as the presence of complex epithelial cell differentiation, that is, adamantinoma-like ES (Bridge et al., 1999), or large cell variants (Folpe et al., 2005; Llombart-Bosch et al., 2009). With the increased application of next generation sequencing and molecular screening, novel genetic alterations were described in tumors resembling ES. Thus *CIC-DUX4* gene fusions and *BCOR-CCNB3* inversions were found in different clinical subsets of SBRCT sharing some but also displaying distinct morphologic and clinical characteristics from classic ES (Kawamura-Saito et al., 2006; Italiano et al., 2012; Pierron et al., 2012).

Although *EWSR1* and FUS belong to the same family of RNA binding proteins and appear to be functionally interchangeable, only rare ES have been reported to date harboring *FUS* gene rearrangements. A novel t(16;21)(p11;q22) translocation was first reported in a small series of four ES cases (Shing et al., 2003), resulting in the fusion of *FUS (fused in sarcoma)* and *ERG (erythroblast transformation specific related)* genes. A number of different fusion transcripts have been reported, fusing one of the *FUS* exons 5–7 to *ERG* exon 6–9 (Shing et al., 2003; Berg et al., 2009). Subsequently, a t(2;16) translocation resulting in an in-frame fusion of *FUS-FEV* was reported (Ng et al., 2007), involving *FUS* exon 10 to *FEV* exon 2. A second putative case of *FUS-FEV* fusion was detected by transcriptome sequencing and confirmed by RT-PCR (Pierron et al., 2012), but the exact fusion transcript was not disclosed. More recently a novel *FUS-NFATC2* fusion was detected by RNA sequencing in a large genomic study of Ewing sarcoma, in which *FUS* exon 6 was fused to exon 2 of *NFATC2* (Brohl et al., 2014). This novel fusion occurred in a 15-year-old male with a femur lesion; its morphologic description included some atypical features, such as focal areas of spindling as well as foci of chondroid differentiation. However, no previous study to date has investigated the incidence of *FUS* gene abnormalities in a molecularly well-characterized cohort of ES. Furthermore, since most of the reported *FUS*-rearranged SBRCTs have a limited pathologic description, it is not known if the clinical and pathologic features of these cases overlap with the classic ES with *EWSR1-FLI1* fusion.

Our findings confirm the rarity of *FUS* gene rearrangements in ES, with only seven (8.2%) cases harboring this genetic abnormality among 85 SBRCTs negative for all other known

fusions. Our results further confirm that *ERG* is the most common ETS member partner participating in the fusion, a *FUS-ERG* fusion being detected in 6/7 cases. Only one SBRCT with *FUS-FEV* fusion was identified, occurring in a skeletal location of a young adult.

Compared to the eight reported cases, the patients from our series of seven *FUS*-rearranged ESs were older (median age at diagnosis of 31 years versus 15 years in the literature) and occurred preferentially in women compared to equal gender distribution. Furthermore the tumors in our study were evenly distributed between bone and soft tissue, while the reported cases occurred predominantly in the bone. No other significant differences were discerned in their morphologic appearance or immunoprofile. Combining our current series to the reported data, there are 11 *FUS-ERG* positive ESs, eight of them occurring in the bone, two in soft tissue and one in the kidney. Cumulative patient data revealed a median age of 15 years (mean 20; range 3–46), with an overall female predominance (73% of patients). Morphologically both the reported and our *FUS-ERG* fusion positive SBRCTs had a monomorphic round cell cytomorphology in keeping with a classic ES phenotype. Furthermore, tumors showed diffuse membranous CD99 reactivity in all except one case, which showed a patchy staining pattern. Moreover, compared to the *EWSR1-ERG* fusion positive ES there was no difference noted in the age at presentation, gender, anatomic location and morphologic appearance. Similarly, all *EWSR1-ERG* ES demonstrated diffuse CD99 membranous staining.

The presence of diffuse and strong CD99 membranous pattern of staining in a SBRCT with a typical morphology reminiscent of ES but with FISH negative for *EWSR1* rearrangement, should raise suspicion for the possibility of *FUS-ERG* fusion. In contrast, other *EWSR1*-negative SBRCTs with alternative fusions, such as *CIC-DUX4* or *BCOR-CCNB3*, more often exhibit patchy CD99 positivity (Fisher, 2014; Puls et al., 2014). In the case of *CIC-DUX4* positive SBRCTs the morphologic appearance is less monomorphic, with prominent nucleoli, more abundant cytoplasm and often myxoid stroma (Italiano et al., 2012). Furthermore, one of our cases showed FLI1 immunopositivity; aberrant FLI1 expression has been previously described in rare ES cases with *EWSR1-ERG* fusion (Folpe et al., 2005).

In the process of our investigation we identified a group of *ERG*-rearranged ES, lacking FISH abnormalities in either *EWSR1* or *FUS* genes. The RNA sequencing performed in one case confirmed the presence of an *EWSR1-ERG* fusion transcript, suggesting an unbalanced, complex rearrangement beyond the FISH resolution. These results are in keeping with the few prior reports demonstrating a complex and unbalanced exchange of chromosomal material between chromosomes 21 and 22 (Desmaze et al., 1997; Szuhai et al., 2006). It was previously reported by FISH and RT-PCR that the chromosome 22 fragment containing the 5′ portion of *EWSR1* is inverted and inserted into chromosome 21, fusing to the 3′; portion of *ERG*; this finding being often not visible on routine cytogenetics (Kaneko et al., 1997). In their study, the two color fusion assay FISH showed that *EWSR1* and *ERG* clones fuse signals on the der(21) chromosome, but no *ERG* signals on the chromosome 22 homologs. Since the t(21;22) in Ewing sarcomas are mostly unbalanced, the size of the inversion/insertion chromosomal segment transferred between chromosomes 21 and 22 is variable in size and often quite small, it is not surprising that *EWSR1-ERG* fusion is often masked, beyond the resolution of routine cytogenetics, and in some cases even beyond the

FISH break-apart resolution according to our results. As these two genes have opposite orientations, this complex pattern of rearrangement and subsequent inversion is required for a functional transcript to occur. In contrast, *EWSR1-FLI1* or *FUS-ERG* fusions typically result from simple balanced translocation events, as the gene partners have similar directions of transcription. In this study, the *EWSR1-ERG* fusion was confirmed by a fusion FISH assay in all four SBRCTs with *ERG* gene rearrangements and negative break-apart FISH for *EWSR1* and *FUS* abnormalities. Due to its relatively low-cost, low failure rates and a 24-hour turn-around time, FISH testing has gained a wide applicability recently in the translocation work-up of sarcomas, replacing most other more laborious molecular techniques, such as conventional karyotyping and RT-PCR, especially in small biopsy material or when only archival material is available. Thus *EWSR1* gene status as reflected by a single FISH assay has nowadays too often become the first and last resource in confirming the diagnosis of ES at the molecular level. Our results show that in the setting of *EWSR1-ERG* fusions, standard break-apart FISH for *EWSR1* will yield false negative results in half of the cases as a consequence of the complex rearrangement pattern between these two genes with inverse orientations, requiring often a multistep mechanism, with multiple, unbalanced breaks, inversions and insertions events (Desmaze et al., 1997; Maire et al., 2008). Thus other molecular techniques, that is, RT-PCR or NGS designed to span known fusion breakpoints, might be required for a more definitive classification. Alternatively, FISH for *ERG* gene rearrangements and/or 3-color FISH fusion assay for *EWSR1* and *ERG* can be used to prevent this pitfall. We recommend following one of these approaches when dealing with a SBRCT displaying the typical ES monomorphic cytomorphology and diffuse reactivity for both CD99 and ERG.

In the context of SBRCTs, ERG reactivity should be interpreted with caution and only in addition to other supporting evidence for ES diagnosis. ERG immunopositivity has in fact also been described in other SBRCTs, mainly *CIC-DUX4* fusion positive, which often display WT1 and ERG immunoreactivity (Specht et al., 2014). Furthermore, identical *FUS-ERG* fusions have been identified in pediatric acute myelocytic leukemia, and ERG-immunopositive leukemic soft tissue infiltrates may suggest a diagnosis of *ERG*-rearranged SBRCT and should be interpreted in the context of other leukemia markers, such as CD43 and myeloperoxidase (Choi et al., 2006). Moreover, high grade undifferentiated angiosarcomas with an epithelioid to small blue round cell phenotype strongly express ERG immunoreactivity and may lack any vasoformative properties. Thus adding CD31 immunostaining is required for any ERG-positive neoplasm, since CD31 is a highly reliable endothelial marker in angiosarcoma and has more specificity compared to ERG in this context.

In conclusion, our study is the first molecular investigation to establish the prevalence of *FUS* gene rearrangements in a well-characterized cohort of SBRCT, which accounts for 8.2% of cases lacking all other known fusions. The most common *FUS* gene partner is *ERG*, with very infrequent cases showing *FEV* gene involvement. *FUS-ERG* positive SBRCTs show a monotonous morphologic phenotype and strong CD99 membranous immunoreactivity, which are similar to classic ES. We suggest that FISH for *FUS* gene rearrangements should be examined in *EWSR1* negative SBRCTs with classic histology and membranous CD99 immunopositivity. Our study also highlights a significant pitfall in the

setting of *EWSR1-ERG* fusion SBRCTs, where FISH assay may not be able to detect the *EWSR1* gene rearrangements due to the complex pattern of t(21;22) translocation. These results also caution interpreting discrepant molecular results from the overall morphologic and immunohistochemical findings. As detection of *EWSR1* break-apart by FISH is emerging as the gold standard for diagnosis of ES, these results raise awareness to the use of a single method in the molecular diagnosis of complex gene rearrangements.

Supplementary Material

Refer to Web version on PubMed Central for supplementary material.

ACKNOWLEDGMENTS

The authors are grateful to Drs. Noah Federman, Department of Pediatric Oncology, and Fritz Eilber, Department of Surgery, UCLA, for providing clinical follow-up; and Milagros Soto, MSKCC, for editorial assistance.

Supported by: Cancer Center Support Grant of the National Institute of Health/National Cancer Institute, Grant numbers: P50 CA140146-01 and P30 CA008748 (to CRA); Kristen Ann Carr Foundation (to CRA).

REFERENCES

Antonescu C. Round cell sarcomas beyond Ewing: Emerging entities. Histopathology. 2014; 64:26–37. [PubMed: 24215322]

Antonescu CR, Zhang L, Chang NE, Pawel BR, Travis W, Katabi N, Edelman M, Rosenberg AE, Nielsen GP, Dal Cin P, Fletcher CD. EWSR1-POU5F1 fusion in soft tissue myoepithelial tumors. A molecular analysis of sixty-six cases, including soft tissue, bone, and visceral lesions, showing common involvement of the EWSR1 gene. Genes Chromosomes Cancer. 2010; 49:1114–1124. [PubMed: 20815032]

Berg T, Kalsaas AH, Buechner J, Busund LT. Ewing sarcoma-peripheral neuroectodermal tumor of the kidney with a FUS-ERG fusion transcript. Cancer Genet Cytogenet. 2009; 194:53–57. [PubMed: 19737655]

Bridge JA, Fidler ME, Neff JR, Degenhardt J, Wang M, Walker C, Dorfman HD, Baker KS, Seemayer TA. Adamantinoma-like Ewing's sarcoma: Genomic confirmation, phenotypic drift. Am J Surg Pathol. 1999; 23:159–165. [PubMed: 9989842]

Brohl AS, Solomon DA, Chang W, Wang J, Song Y, Sindiri S, Patidar R, Hurd L, Chen L, Shern JF, Liao H, Wen X, Gerard J, Kim JS, Lopez Guerrero JA, Machado I, Wai DH, Picci P, Triche T, Horvai AE, Miettinen M, Wei JS, Catchpool D, Llombart-Bosch A, Waldman T, Khan J. The genomic landscape of the Ewing Sarcoma family of tumors reveals recurrent STAG2 mutation. PLoS Genet. 2014; 10:e1004475. [PubMed: 25010205]

Choi HW, Shin MG, Sawyer JR, Cho D, Kee SJ, Baek HJ, Kook H, Kim HJ, Shin JH, Suh SP, Hwang TJ, Ryang DW. Unusual type of TLS/FUS-ERG chimeric transcript in a pediatric acute myelocytic leukemia with 47,XX,110,t(16;21)(p11; q22). Cancer Genet Cytogenet. 2006; 167:172–176. [PubMed: 16737920]

Delattre O, Zucman J, Plougastel B, Desmaze C, Melot T, Peter M, Kovar H, Joubert I, de Jong P, Rouleau G, et al. Gene fusion with an ETS DNA-binding domain caused by chromosome translocation in human tumours. Nature. 1992; 359:162–165. [PubMed: 1522903]

Delattre O, Zucman J, Melot T, Garau XS, Zucker JM, Lenoir GM, Ambros PF, Sheer D, Turc-Carel C, Triche TJ, et al. The Ewing family of tumors–a subgroup of small-round-cell tumors defined by specific chimeric transcripts. N Engl J Med. 1994; 331:294–299. [PubMed: 8022439]

Desmaze C, Brizard F, Turc-Carel C, Melot T, Delattre O, Thomas G, Aurias A. Multiple chromosomal mechanisms generate an EWS/FLI1 or an EWS/ERG fusion gene in Ewing tumors. Cancer Genet Cytogenet. 1997; 97:12–19. [PubMed: 9242212]

Dobin A, Davis CA, Schlesinger F, Drenkow J, Zaleski C, Jha S, Batut P, Chaisson M, Gingeras TR. STAR: Ultrafast universal RNA-seq aligner. Bioinformatics. 2013; 29:15–21. [PubMed: 23104886]

Ewing J. Diffuse endothelioma of bone. Proc NY Path Soc. 1921; 21:17–24.

Fisher C. The diversity of soft tissue tumours with EWSR1 gene rearrangements: A review. Histopathology. 2014; 64:134–150. [PubMed: 24320889]

Folpe AL, Goldblum JR, Rubin BP, Shehata BM, Liu W, Dei Tos AP, Weiss SW. Morphologic and immunophenotypic diversity in Ewing family tumors: A study of 66 genetically confirmed cases. Am J Surg Pathol. 2005; 29:1025–1033. [PubMed: 16006796]

Ginsberg JP, de Alava E, Ladanyi M, Wexler LH, Kovar H, Paulussen M, Zoubek A, Dockhorn-Dworniczak B, Juergens H, Wunder JS, Andrulis IL, Malik R, Sorensen PH, Womer RB, Barr FG. EWS-FLI1 and EWS-ERG gene fusions are associated with similar clinical phenotypes in Ewing's sarcoma. J Clin Oncol. 1999; 17:1809–1814. [PubMed: 10561219]

Habegger L, Sboner A, Gianoulis TA, Rozowsky J, Agarwal A, Snyder M, Gerstein M. RSEQtools: A modular framework to analyze RNA-Seq data using compact, anonymized data summaries. Bioinformatics. 2011; 27:281–283. [PubMed: 21134889]

Italiano A, Sung YS, Zhang L, Singer S, Maki RG, Coindre JM, Antonescu CR. High prevalence of CIC fusion with double-homeobox (DUX4) transcription factors in EWSR1-negative undifferentiated small blue round cell sarcomas. Genes Chromosomes Cancer. 2012; 51:207–218. [PubMed: 22072439]

Jeon IS, Davis JN, Braun BS, Sublett JE, Roussel MF, Denny CT, Shapiro DN. A variant Ewing's sarcoma translocation (7;22) fuses the EWS gene to the ETS gene ETV1. Oncogene. 1995; 10:1229–1234. [PubMed: 7700648]

Kaneko Y, Yoshida K, Handa M, Toyoda Y, Nishihira H, Tanaka Y, Sasaki Y, Ishida S, Higashino F, Fujinaga K. Fusion of an ETS-family gene, EIAF, to EWS by t(17;22)(q12;q12) chromosome translocation in an undifferentiated sarcoma of infancy. Genes Chromosomes Cancer. 1996; 15:115–121. [PubMed: 8834175]

Kaneko Y, Kobayashi H, Handa M, Satake N, Maseki N. EWS-ERG fusion transcript produced by chromosomal insertion in a Ewing sarcoma. Genes Chromosomes Cancer. 1997; 18:228–231. [PubMed: 9071576]

Kawamura-Saito M, Yamazaki Y, Kaneko K, Kawaguchi N, Kanda H, Mukai H, Gotoh T, Motoi T, Fukayama M, Aburatani H, Takizawa T, Nakamura T. Fusion between CIC and DUX4 up-regulates PEA3 family genes in Ewing-like sarcomas with t(4;19)(q35;q13) translocation. Hum Mol Genet. 2006; 15:2125–2137. [PubMed: 16717057]

Llombart-Bosch A, Blache R, Peydro-Olaya A. Ultrastructural study of 28 cases of Ewing's sarcoma: Typical and atypical forms. Cancer. 1978; 41:1362–1373. [PubMed: 346195]

Llombart-Bosch A, Machado I, Navarro S, Bertoni F, Bacchini P, Alberghini M, Karzeladze A, Savelov N, Petrov S, Alvarado-Cabrero I, Mihaila D, Terrier P, Lopez-Guerrero JA, Picci P. Histological heterogeneity of Ewing's sarcoma/PNET: An immunohistochemical analysis of 415 genetically confirmed cases with clinical support. Virchows Arch. 2009; 455:397–411. [PubMed: 19841938]

Maire G, Brown CW, Bayani J, Pereira C, Gravel DH, Bell JC, Zielenska M, Squire JA. Complex rearrangement of chromosomes 19, 21, and 22 in Ewing sarcoma involving a novel reciprocal inversion-insertion mechanism of EWS-ERG fusion gene formation: A case analysis and literature review. Cancer Genet Cytogenet. 2008; 181:81–92. [PubMed: 18295659]

Mastrangelo T, Modena P, Tornielli S, Bullrich F, Testi MA, Mezzelani A, Radice P, Azzarelli A, Pilotti S, Croce CM, Pierotti MA, Sozzi G. A novel zinc finger gene is fused to EWS in small round cell tumor. Oncogene. 2000; 19:3799–3804. [PubMed: 10949935]

Ng TL, O'Sullivan MJ, Pallen CJ, Hayes M, Clarkson PW, Winstanley M, Sorensen PH, Nielsen TO, Horsman DE. Ewing sarcoma with novel translocation t(2;16) producing an in-frame fusion of FUS and FEV. J Mol Diagn. 2007; 9:459–463. [PubMed: 17620387]

Peter M, Couturier J, Pacquement H, Michon J, Thomas G, Magdelenat H, Delattre O. A new member of the ETS family fused to EWS in Ewing tumors. Oncogene. 1997; 14:1159–1164. [PubMed: 9121764]

Pierron G, Tirode F, Lucchesi C, Reynaud S, Ballet S, Cohen-Gogo S, Perrin V, Coindre JM, Delattre O. A new sub-type of bone sarcoma defined by BCOR-CCNB3 gene fusion. Nat Genet. 2012; 44:461–466. [PubMed: 22387997]

Puls F, Niblett A, Marland G, Gaston CL, Douis H, Mangham DC, Sumathi VP, Kindblom LG. BCOR-CCNB3 (Ewing-like) sarcoma: A clinicopathologic analysis of 10 cases, in comparison with conventional Ewing sarcoma. Am J Surg Pathol. 2014; 38:1307–1318. [PubMed: 24805859]

Quail MA, Kozarewa I, Smith F, Scally A, Stephens PJ, Durbin R, Swerdlow H, Turner DJ. A large genome center's improvements to the Illumina sequencing system. Nat Methods. 2008; 5:1005–1010. [PubMed: 19034268]

Sboner A, Habegger L, Pflueger D, Terry S, Chen DZ, Rozowsky JS, Tewari AK, Kitabayashi N, Moss BJ, Chee MS, Demichelis F, Rubin MA, Gerstein MB. FusionSeq: A modular framework for finding gene fusions by analyzing paired-end RNA-sequencing data. Genome Biol. 2010; 11:R104. [PubMed: 20964841]

Shing DC, McMullan DJ, Roberts P, Smith K, Chin SF, Nicholson J, Tillman RM, Ramani P, Cullinane C, Coleman N. FUS/ERG gene fusions in Ewing's tumors. Cancer Res. 2003; 63:4568–4576. [PubMed: 12907633]

Specht K, Sung YS, Zhang L, Richter GH, Fletcher CD, Antonescu CR. Distinct transcriptional signature and immunoprofile of CIC-DUX4 fusion-positive round cell tumors compared to EWSR1-rearranged Ewing sarcomas: Further evidence toward distinct pathologic entities. Genes Chromosomes Cancer. 2014; 53:622–633. [PubMed: 24723486]

Sumegi J, Nishio J, Nelson M, Frayer RW, Perry D, Bridge JA. A novel t(4;22)(q31;q12) produces an EWSR1-SMARCA5 fusion in extraskeletal Ewing sarcoma/primitive neuroectodermal tumor. Mod Pathol. 2011; 24:333–342. [PubMed: 21113140]

Szuhai K, Ijszenga M, Tanke HJ, Rosenberg C, Hogendoorn PC. Molecular cytogenetic characterization of four previously established and two newly established Ewing sarcoma cell lines. Cancer Genet Cytogenet. 2006; 166:173–179. [PubMed: 16631476]

Szuhai K, Ijszenga M, de Jong D, Karseladze A, Tanke HJ, Hogendoorn PC. The NFATc2 gene is involved in a novel cloned translocation in a Ewing sarcoma variant that couples its function in immunology to oncology. Clin Cancer Res. 2009; 15:2259–2268. [PubMed: 19318479]

Wang L, Bhargava R, Zheng T, Wexler L, Collins MH, Roulston D, Ladanyi M. Undifferentiated small round cell sarcomas with rare EWS gene fusions: Identification of a novel EWS-SP3 fusion and of additional cases with the EWS-ETV1 and EWS-FEV fusions. J Mol Diagn. 2007; 9:498–509. [PubMed: 17690209]

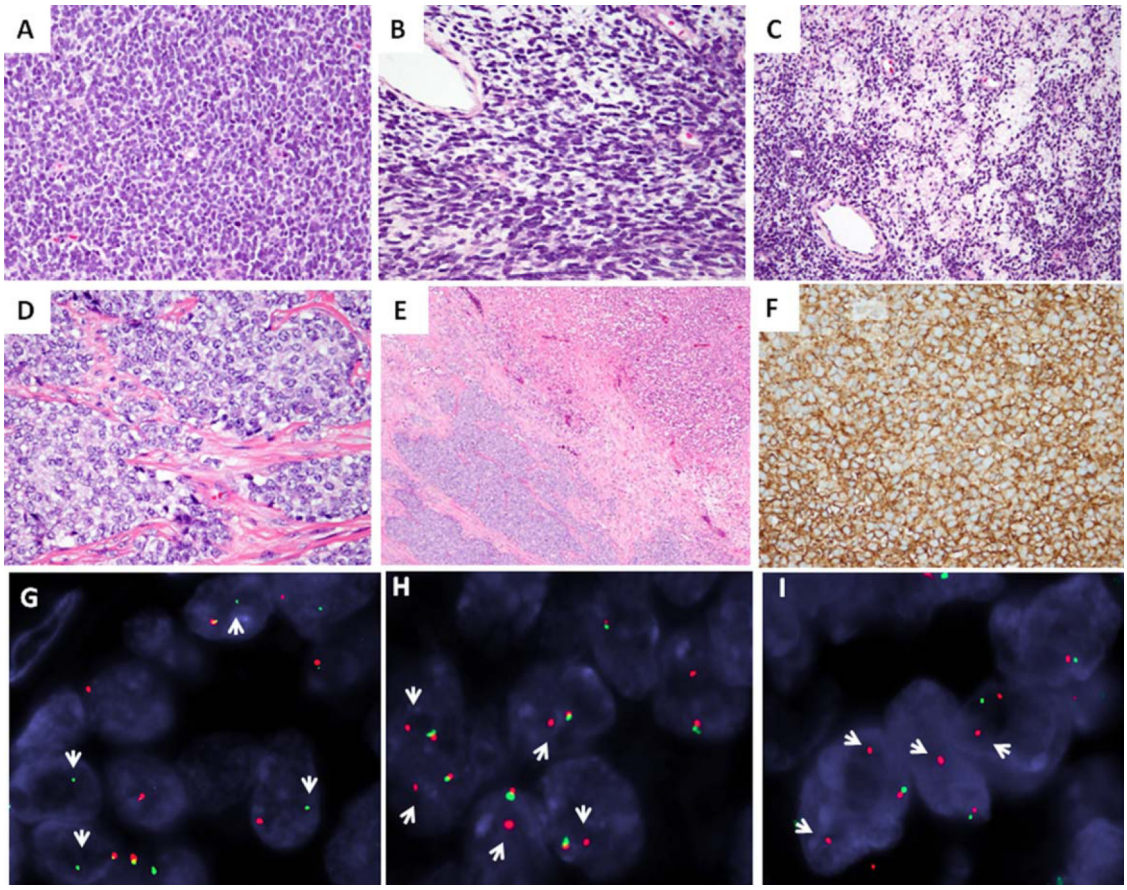

Figure 1.

The morphologic spectrum and FISH gene rearrangements in Ewing sarcoma with *FUS* gene abnormalities. *FUS-ERG* positive tumor characterized by solid growth of primitive, small blue cells with diffuse hyperchromasia and scant cytoplasm (A, ES1), focal areas of spindling and myxoid changes (B, C, ES1); Another *FUS-ERG* tumor with vesicular chromatin and vacuolated cytoplasm, separated in nests and compartments by fibrous bands and geographic areas of necrosis (D, E, ES2); All cases showed crisp and diffuse membranous staining pattern for CD99 (F, ES3); FISH break-apart assay showing unbalanced rearrangements for *FUS* (G, loss of red centromeric signal; ES2), *ERG* (H, loss of green telomeric signal; ES2), and *FEV* (I; loss of green telomeric signal; ES4) (red, centromeric, green, telomeric; arrows break-apart signals). [Color figure can be viewed in the online issue, which is available at wileyonlinelibrary.com.]

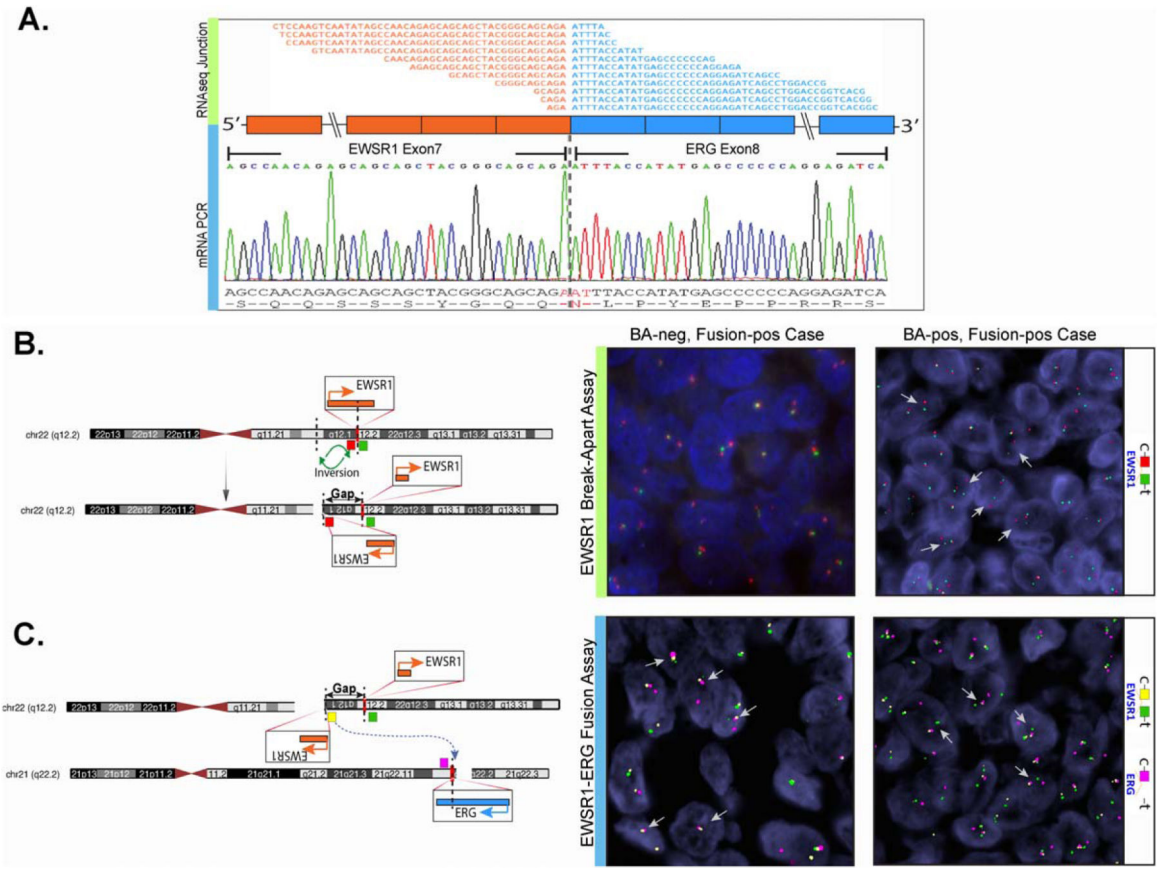

Figure 2.

Complex or masked gene rearrangements in Ewing sarcomas with *EWSR1-ERG* fusions. A. RNA sequencing (upper panel, fusion junction reads) and RT-PCR (lower panel) confirmation of *EWSR1-ERG* fusion (exon 7 of *EWSR1* fused to exon 8 of *ERG*) in ES17. B. Diagrammatic representation of the multistep, complex mechanism of unbalanced t(21;22) translocation, with one such example involving two 22q12 breaks, including the *EWSR1* break, followed by inversion; depending on the size of the inverted segment (gap, green arrows), the *EWSR1* FISH break-apart might not (central panel, ES17) or may (right panel, ES23) be positive (red, centromeric; green, telomeric). C. The 5′*EWSR1* fragment insertion on derivative 21, schematic depiction (left) and 3-color FISH fusion assay confirming the association of 5′*EWSR1* orange centromeric signal with the red *ERG* signal (central and right panels, ES17 and ES23)(green, *EWSR1* telomeric). [Color figure can be viewed in the online issue, which is available at wileyonlinelibrary.com.]

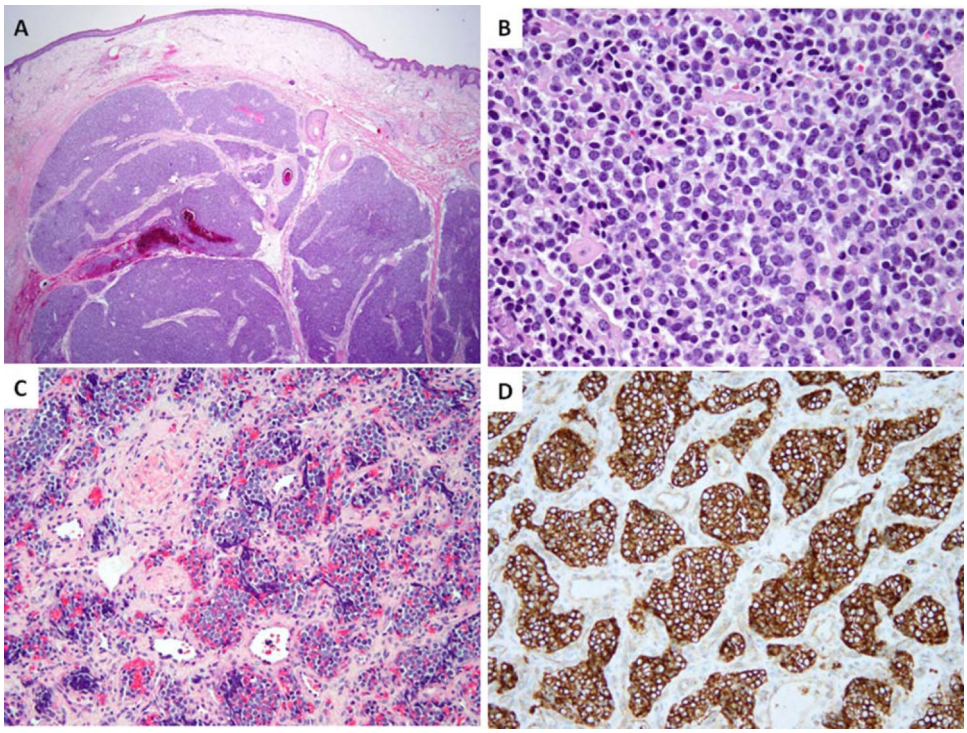

Figure 3.

Morphologic spectrum of EWSR1-ERG Ewing sarcomas. Nodular growth of ES involving deep dermis and subcutis of the scalp (A, ES22); solid growth showing ill-defined cell borders and round nuclei with fine chromatin (B, ES17); a distinctive nested growth in an infant with ES from the vertebral body, showing diffuse CD99 reactivity (C, D; ES16). [Color figure can be viewed in the online issue, which is available at wileyonlinelibrary.com.]

TABLE 1

Clinicopathologic Features of *FUS* Rearranged SBRCT From Our Study and Literature Review

Present study/Reference	Age/gender	Site	CD99	FUS-fusiontypeby FISH	Follow-up (months)
ES1	31/F	Thigh	Diffuse membranous	FUS-ERG	NED (16)
ES2	15/F	Femur	Diffuse membranous	FUS-ERG	NED (12)
ES3	46/F	Chest wall	Diffuse membranous	FUS-ERG	NED (5)
ES4	46/F	Arm	Diffuse membranous	FUS-FEV	AWD (24) Lung mets
ES5	13/F	Ilium	Diffuse membranous	FUS-ERG	–
ES6	45/M	Chest wall	Diffuse membranous	FUS-ERG	AWD (12) Lung mets
ES7	19/F	Thigh	Diffuse membranous	FUS-ERG	–
ES8 (Shing et al., 2003)	9/M	Chest wall	Membranous	FUS-ERG	DOD (24)
ES9 (Shing et al., 2003)	7/F	Chest wall	Patchy membranous	FUS-ERG	–
ES10 (Shing et al., 2003)	15/F	Chest wall	Membranous	FUS-ERG	–
ES11 (Shing et al., 2003)	21/M	Femur	Membranous	FUS-ERG	–
ES12 (Berg et al., 2009)	3/F	Kidney	Strong membranous	FUS-ERG	NED (16)
ES13 (Pierron et al., 2012)	–	–	–	FUS-FEV	–
ES14 (Ng et al., 2007)	33/M	Clavicle	Strong membranous	FUS-FEV	NED (10)
ES15 (Brohl et al., 2014)	15/M	Femur	–	FUS-NFATC2	–

M, male; F, female; DOD, dead of disease at the time of publication; NED, no evidence of disease.

TABLE 2

Clinicopathologic Features of the *EWSR1-ERG* Positive Ewing Sarcoma

Patient	Age/gender	Site	ERG IHC	CD99 IHC	FUS FISH	FISH EWS	FISH ERG	Follow-up (months)
ES16	1/F	T10	Diffuse	Diffuse membranous	ND	Positive[a]	Positive	NED (27)
ES17	16/F	Ilium	Diffuse	Diffuse membranous	Negative	Negative[b]	Positive	NED (6)
ES18	4/F	Retro-peritoneum	Diffuse	Diffuse membranous	ND	Positive	Positive	AWD (2)
ES19	22/M	Mandible	Diffuse	Diffuse membranous	Negative	Negative[c]	Positive	–
ES20	23/M	Brain	Diffuse	Diffuse membranous	Negative	Negative	Positive	LFU (6)
ES21	19/F	Chest wall	ND	Diffuse membranous	Negative	Negative	Positive	AWD (16)
ES22	20/F	Scalp	Diffuse	Diffuse membranous	ND	Positive	Positive	NED (9)
ES23	22/F	Intra-abdominal	Diffuse	Diffuse membranous	Negative	Positive	Positive	NED (4)

[a] FISH detected only 4% of cells with standard pattern and an additional 10% with complex rearrangement (loss of *3'EWSR1* or duplication of rear-ranged *EWSR1).*

[b] *EWSR1-ERG* fusion was confirmed by RNAseq, and subsequently validated by ERG FISH.

[c] ERG FISH was done due to ERG IHC positivity in the absence of *EWSR1* rearrangement by FISH; NED: No evidence of disease; LFU: Lost to follow up; AWD: Alive with disease.